

Numerical study of Natural Convection of Magnetic Fluids in a Cubic Cavity with a Heat Generating Object Inside by the Lattice Boltzmann Method

Xiao-Dong Niu^{1,*}, Hiroshi Yamaguchi¹, Xin-Rong Zhang^{2,1} and Keisuke Yoshikawa¹

¹ Energy Conversion Research Center, Department of Mechanical Engineering, Doshisha University, Kyoto 630-0321, Japan

² Department of Energy and Resources Engineering, College of Engineering, Peking University, 100871, P. R. China

Received 21 May 2009; Accepted (in revised version) 02 July 2009

Available online 31 December 2009

Abstract. In this article, natural convection of a magnetic fluid in a cubic cavity with a heat generating object inside and under a uniform magnetic field is simulated by the lattice Boltzmann method. Results obtained from the present simulations are shown to be agreed well with our experimental measurements, and reveal more of effects of the magnetic field on the flow and heat transfer of the magnetic fluids.

PACS: 47.65.cb

Key words: Magnetic fluids, natural convection, Lattice Boltzmann method.

1 Introduction

Magnetic fluids are super paramagnetic fluids formed by a stable colloidal suspension of ferromagnetic nanoparticles dispersed in carrier liquids such as water or kerosene [1]. Among various magnetic fluids, there is a so-called temperature-sensitive magnetic fluid (TSMF), whose magnetization strongly depends on the temperature. Becau-

*Corresponding author.

URL: <https://kenkyudb.doshisha.ac.jp/rd/search/researcher/108197/index-j.html>

Email: xniu@mail.doshisha.ac.jp (X.-D. Niu), hyamaguc@mail.doshisha.ac.jp (H. Yamaguchi), xrzhang@coe.pku.edu.cn (X.-R. Zhang), dth0319@mail4.doshisha.ac.jp (K. Yoshikawa)

se of its being operated easily in the room temperature range, the TSMF is considered as a promising fluid in energy conversion and heat transport systems with small length scale or under microgravity environment [2, 3]. Due to the important role of the convection mechanism in the energy conversion and heat transportation, a thorough understanding of relations between the applied magnetic field and the resulted convection is necessary.

Flow behaviors as well as the heat transfer characteristics associated with the natural convection of the TSMF have been studied by many researchers in the past years [4–8]. Finlayson [4] first studied the thermomagnetic convection of the TSMF and showed that there exists a critical parameter beyond which the thermomagnetic convection occurs. Schwab et al. [5] conducted an experimental investigation of the convective instability in a horizontal layer of the TSMF and characterized the influence of the magnetic Rayleigh number on the Nusselt number. Krakov and Nikiforov [6] addressed the influences of the relative orientation of the temperature gradient and the magnetic field on thermomagnetic convection in a square cavity. Yamaguchi et al. [7, 8] performed experiments and numerical analyses in a square enclosure and characterized the heat transfer in terms of the magnetic Rayleigh number.

However, in most of practical situations, a container with heat generating objects inside is often encountered, and studying the convection of such a case is fewer but nontrivial in both academics and engineering. For this reason, in our recent study [9], the natural convection of the TSMF in a cubic container with a heat generating square cylinder object inside was investigated under a uniform magnetic field experimentally. The experimental results showed that the heat transfer characteristic of the TSMF is enhanced when the magnetic field is applied. The stronger the magnetic field, the better the heat transfer characteristic can be achieved.

As a compensation of the above experimental research, and in order to disclose more physics behind the experimental findings, in this paper the natural convection of the TSMF in a cubic cavity with a heat generating object inside under a uniform magnetic field is numerically carried out by using the lattice Boltzmann method (LBM) [10, 11]. The LBM [10, 11] is formulated based on a derived scalar magnetic potential advection-diffusion equation at the first-order time accuracy. By defining an effective velocity, which is a function of the temperature gradient, a lattice Boltzmann scheme for the magnetic field is straightforwardly constructed in a similar fashion of that of modeling the temperature transport equation. To ensure the scheme close to the original elliptic scalar potential equation, the time derivative in the advection-diffusion equation is multiplied by an adjustable preconditioning parameter. In the present study, using the LBM [10, 11], we particularly focus on investigating the effects of the magnetic field on the characteristics of the flow and heat transfer as well as the temperature behaviors in the considered flow field.

The rest of the paper is organized as follows. In Section 2, the LBM [10, 11] with numerical implementations is introduced briefly. Section 3 is devoted to results and discussions of the present study. The results obtained are compared to experimental measurements conducted in our labs. A conclusion is given in Section 4.

2 Methodology and numerical implementations

2.1 Lattice Boltzmann models

In the theory of the magnetic fluids, as the flow under influences of the magnetic field, it undergoes magnetic force. The magnetic hydrodynamics for the non-conductive magnetic fluid can be described by the following governing equations (2.1)-(2.2)

$$\partial_t \rho + \nabla \rho_0 \mathbf{u} = 0, \quad (2.1)$$

$$\begin{aligned} & \rho_0 [\partial_t (\mathbf{u}) + (\mathbf{u} \cdot \nabla) \mathbf{u}] \\ = & -\nabla p + \eta \left[\nabla^2 \mathbf{u} + \frac{1}{3} \nabla (\nabla \cdot \mathbf{u}) \right] + \mu_0 \mathbf{M} \cdot \nabla \mathbf{H} - \rho \beta (T - T_0) \mathbf{g}, \end{aligned} \quad (2.2)$$

$$\begin{aligned} & \left[\rho_0 C_p - \mu_0 \mathbf{H} \cdot \left(\frac{\partial \mathbf{M}}{\partial T} \right)_H \right] (\partial_t T + \mathbf{u} \cdot \nabla T) \\ = & \lambda \nabla^2 T - \left(\mu_0 T \left(\frac{\partial \mathbf{M}}{\partial T} \right)_H \cdot \frac{D \mathbf{H}}{D t} \right), \quad \text{Fluid,} \end{aligned} \quad (2.3)$$

$$\rho_H C_{pH} \partial_t T = \lambda_H \nabla^2 T, \quad \text{Heat generating object,} \quad (2.4)$$

$$\left(1 + \frac{M}{H} \right) \nabla^2 \phi - \left(\frac{M}{H} \right) \cdot \nabla \phi = 0. \quad (2.5)$$

In the above equations, ρ_0 is the constant density, \mathbf{u} is the velocity, p is the pressure, and T is the temperature; η is the dynamical viscosity, μ_0 is the magnetic permeability of vacuum, β is the expansion coefficient under the Boussinesq approximation; H is the modulus of the magnetic intensity \mathbf{H} and ϕ is the scalar potential and $\nabla \phi = \mathbf{H}$ for the non-conductive magnetic fluid; M is the modulus of the magnetization \mathbf{M} ; ϕ is the scalar potential and $\nabla \phi = \mathbf{H}$; λ and λ_H are the coefficients of thermal conductivity of the fluid and the heat generating object, respectively, C_p and C_{pH} are the specific heats of respective fluid and the heat generating object at constant pressure.

In terms of the lattice Boltzmann theory, Eqs. (2.1)-(2.5) can be solved by the following lattice Boltzmann scheme by employing three distribution functions for velocity, thermal and magnetic field [10, 11], respectively, as

$$\begin{aligned} & f_\alpha (\mathbf{r} + \xi_\alpha \delta_t, t + \delta_t) - f_\alpha (\mathbf{r}, t) \\ = & -\frac{f_\alpha (\mathbf{r}, t) - f_\alpha^{eq} (\mathbf{r}, t)}{\tau_f} + w_\alpha \frac{(\tau_f - 0.5) \delta_t}{\tau_f c_s^2} \mathbf{F} \cdot (\xi_\alpha - \mathbf{u}), \end{aligned} \quad (2.6)$$

$$g_\alpha (\mathbf{r} + \xi_\alpha \delta_t, t + \delta_t) - g_\alpha (\mathbf{r}, t) = -\frac{g_\alpha (\mathbf{r}, t) - g_\alpha^{eq} (\mathbf{r}, t)}{\tau_g} + w_\alpha S \delta_t, \quad (2.7)$$

$$h_\alpha (\mathbf{r} + \xi_\alpha \delta_t, t + \delta_t) - h_\alpha (\mathbf{r}, t) = -\frac{h_\alpha (\mathbf{r}, t) - h_\alpha^{eq} (\mathbf{r}, t)}{\tau_h}, \quad (2.8)$$

with the equilibrium distribution functions defined as

$$f_\alpha^{eq} (\mathbf{r}, t) = w_\alpha \left\{ \rho + \rho_0 \left[\frac{\xi_\alpha \cdot \mathbf{u}}{c_s^2} + \frac{1}{2c_s^2} \left(\frac{(\xi_\alpha \cdot \mathbf{u})^2}{c_s^2} - \mathbf{u}^2 \right) \right] \right\}, \quad (2.9)$$

$$g_\alpha^{eq}(\mathbf{r}, t) = w_\alpha T \left\{ 1 + \frac{\tilde{\zeta}_\alpha \cdot \mathbf{u}}{c_s^2} + \frac{1}{2c_s^2} \left(\frac{(\tilde{\zeta}_\alpha \cdot \mathbf{u})^2}{c_s^2} - \mathbf{u}^2 \right) \right\}, \quad (2.10)$$

$$h_\alpha^{eq}(\mathbf{r}, t) = w_\alpha \phi \left\{ 1 + \frac{\tilde{\zeta}_\alpha \cdot \gamma \mathbf{u}_T}{c_s^2} + \frac{1}{2c_s^2} \left(\frac{(\tilde{\zeta}_\alpha \cdot \gamma \mathbf{u}_T)^2}{c_s^2} - (\gamma \mathbf{u}_T)^2 \right) \right\}, \quad (2.11)$$

and the force and source term are

$$\mathbf{F} = \mu_0 M \nabla H - \rho_0 \beta (T - T_0) \mathbf{g}, \quad (2.12)$$

$$S = - \frac{\mu_0 T \mathbf{M} \cdot \frac{D\mathbf{H}}{Dt}}{\rho_0 C_P - \mu_0 \mathbf{H} \cdot \left(\frac{\partial \mathbf{M}}{\partial T} \right)_H}, \quad (2.13)$$

where $\mathbf{r} = \mathbf{r}(x, y, z)$ is the spatial vector;

$$\mathbf{u}_T = -\nabla \left(\frac{M}{H} \right) = \frac{\chi_0 \nabla T}{T_c - T_0},$$

is defined as an effective velocity with T_0 and T_c being the reference and Curie temperatures respectively, and χ_0 the magnetization rate at T_0 ; γ is an adjustable preconditioning parameter introduced to ensure that the solution of the LB scheme (2.8) remains close to a solution of the original scalar potential equation (2.5). The relaxation parameters in Eqs. (2.6)-(2.8) are given by

$$\tau_f = \frac{\eta}{\rho_0 c_s^2 \delta_t} + 0.5, \quad (2.14)$$

$$\tau_g = \frac{D}{(D+2)} \frac{\lambda}{\left[\rho_0 C_P - \mu_0 \mathbf{H} \cdot \left(\frac{\partial \mathbf{M}}{\partial T} \right)_H \right] c_s^2 \delta_t} + 0.5, \quad (2.15)$$

$$\tau_h = \frac{\gamma}{c_s^2 \delta_t} \left(1 + \frac{M}{H} \right) + 0.5, \quad (2.16)$$

respectively. In numerical simulation, the value of the preconditioning parameter γ is chosen by setting $\tau_h = 1$.

The sound speed c_s , the weight coefficient w_α and the discrete velocity $\tilde{\zeta}_\alpha$ used in the above LBM scheme can be referred to the discrete velocity model of the D3Q19 for three-dimension (3D) [12]. The density, velocity, and temperature are calculated by

$$\rho = \sum_\alpha f_\alpha, \quad \rho_0 \mathbf{u} = \sum_\alpha f_\alpha \tilde{\zeta}_\alpha + 0.5 \delta_t \mathbf{F}, \quad T = \sum_\alpha g_\alpha, \quad \phi = \sum_\alpha h_\alpha. \quad (2.17)$$

A number of previous researches [12, 13] have shown, by the Chapman-Enskog analysis, the lattice Boltzmann equations (2.6)-(2.8) be capable of recovering to the following macroscopic equations (2.1)-(2.5), respectively.

2.2 Numerical implementation and boundary conditions

The natural convection of the magnetic fluid in a cubic cavity with heat generating object inside under a uniform magnetic field investigated in the present paper is in line with our experimental conditions (Table 1). The cubic cavity has the side length $L=7.5\text{mm}$, and the heat generating stick inside the cavity has the longitude and side lengths of L and $L/3$, respectively. The temperatures on the upper and bottom walls are same and fixed at $T_b=T_u=T_0=298.15\text{K}$.

The evaluation of the heat transfer characteristics of the test TSMF in the container is based on the following parameters:

$$Gr = \frac{\rho_0^2 g \beta \Delta T_{ref} L^3}{\eta_0^2}, \quad Grm = \frac{\rho_0^2 \mu_0 \chi_0 H_0^2 L^2}{\eta_0^2}, \quad Nu = \iint \left(-\frac{\partial T}{\partial Z} \right)_{z=0,L} dx dy, \quad (2.18)$$

where

$$\Delta T_{ref} = T_h - \frac{T_u + T_b}{2},$$

is the representative temperature difference between the heat generating object and the upper/bottom walls, and Gr and Grm are the Grashof and magnetic Grashof numbers, respectively; Nu is an effective Nusselt number. With the grid-independence investigations of other two grids of $25 \times 25 \times 25$ and $43 \times 43 \times 43$ in advance, all the simulations in the present study are carried out on the uniform grid of $37 \times 37 \times 37$ in the range of $0 < Gr < 160$, and the results presented below are given in the non-dimensional form by \mathbf{r}/L , ($U_{ref} = \sqrt{g\beta L \Delta T_{ref}}$) and $T/\Delta T_{ref}$.

The boundary conditions of the macroscopic variables \mathbf{u} , T are sketched in Fig. 1 in non-dimensional form. For the magnetic field, the magnetic potential boundary conditions are set by the magnetic intensity, which are described as follows

$$\left. \frac{\partial \phi}{\partial x} \right|_{x=0,L} = 0, \quad \left. \frac{\partial \phi}{\partial y} \right|_{y=0,L} = 0, \quad \left. \frac{\partial \phi}{\partial z} \right|_{z=0,L} = H. \quad (2.19)$$

Table 1: Cavity dimension, fluid properties used in present study.

Scale length of cavity L (mm)	7.5	Specific heat C_p (J/kgPK)	1.39×10^1
Density ρ_0 (kg/m ³)	1.397×10^3	Expansion coefficient β (1/K)	6.90×10^{-4}
Viscosity η (Pa · s)	1.680×10^{-3}	Curie temperature T_c (K)	477.35
Thermal conductivity λ (W/(m·K))	1.750×10^{-1}	Reference temperature T_0 (K)	298.15
Thermal conductivity λ_H (W/(m·K))	1.11×10^2	Magnetization rate χ_0	0.2650
Permeability of vacuum μ_0 (H/m)	$4\pi \times 10^{-7}$	Gravitational acceleration g (m/s ²)	9.8
Density ρ_H (kg/m ³)	8.52×10^3	Specific heat C_{pH} (J/kg·K)	3.85×10^2

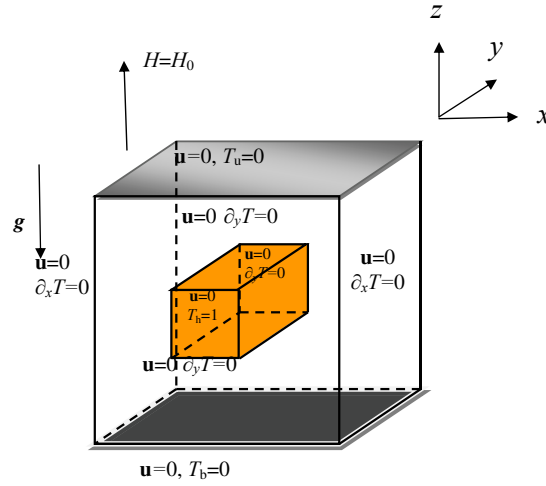


Figure 1: Sketch of the thermal magnetic natural convection flow condition in the cubic cavity.

In our numerical simulation, the temperatures on the isolated walls and the scalar potentials on all walls are calculated based on the second order extrapolation scheme. For the distribution functions of f_{α} , g_{α} and h_{α} on the boundaries, the non-equilibrium bounce back boundary conditions [10] are employed when the macroscopic velocities, temperatures and scalar potentials on the walls are known, and they are given as follows

$$f_{\bar{\alpha}}(\mathbf{r}, t) - f_{\bar{\alpha}}^{eq}(\mathbf{r}, t) = f_{\alpha}(\mathbf{r}, t) - f_{\alpha}^{eq}(\mathbf{r}, t), \tag{2.20}$$

$$g_{\bar{\alpha}}(\mathbf{r}, t) - g_{\bar{\alpha}}^{eq}(\mathbf{r}, t) = - [g_{\alpha}(\mathbf{r}, t) - g_{\alpha}^{eq}(\mathbf{r}, t)], \tag{2.21}$$

$$h_{\bar{\alpha}}(\mathbf{r}, t) - h_{\bar{\alpha}}^{eq}(\mathbf{r}, t) = - [h_{\alpha}(\mathbf{r}, t) - h_{\alpha}^{eq}(\mathbf{r}, t)], \tag{2.22}$$

respectively. $\bar{\alpha}$ in Eqs. (2.20)-(2.22) denotes directions of the unknown distribution function, and $\bar{\alpha} = -\alpha$.

3 Results and discussions

Fig. 2 displays the variations of the average Nusselt numbers on the Grashof numbers at three magnetic Grashof numbers of 0, 1.00×10^4 and 1.96×10^4 . Experimental and numerical results are all plotted in this figure. Seen from Fig. 2, the calculated results are in good agreement with the experimental data [9], and the Nusselt numbers at all three magnetic Grashof numbers increase with the increase of the Grashof number, indicating that the heat transfer rate increases when the magnetic field strength is increased. This observation can be explained more clearly by the following numerical results, which depict details of the flow and magnetic fields.

Fig. 3 shows the velocity vectors of $Gr=75$ inside the cavity at $Grm=1.10 \times 10^4$ (left) and 1.96×10^4 (right). As shown in Fig. 3, four symmetric weak flow rolls occur

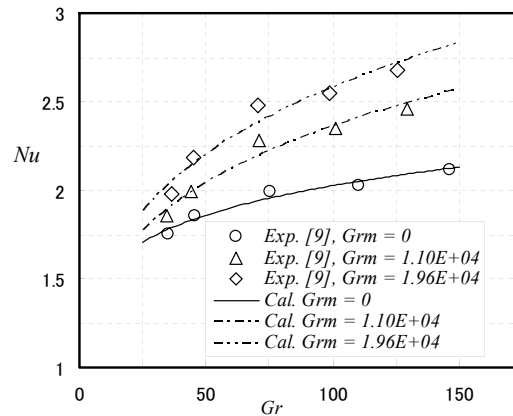


Figure 2: Dependence of the average Nusselt numbers of the Grashof numbers at three magnetic Grashof numbers of 0, 1.10×10^4 and 1.96×10^4 .

near the isolate walls in side cavity due to effects of the magnetic forces. Because the temperature gradient is larger near the heat generating object, the velocity is larger at that region. Moreover, the rolls become stronger with the increase of the magnetic Grashof number. Figs. 4(a) and 4(b) show the flow patterns and temperature fields of $Gr=75$ at four planes of the cavity at $Grm=1.10 \times 10^4$ and 1.96×10^4 , respectively. Corresponding to the velocity field shown in Fig. 3, the low temperature fluid near the upper and bottom cooling walls is brought to the region near the heat generating object, and the high temperature fluid near the heat generating object is brought to the side isolated walls, along which it is further brought to the upper and bottom cooling walls. The heat transport rate is larger at high magnetic Grashof number than that at low magnetic Grashof number. As shown in Figs. 4(a) with 4(b), it can also be observed that the heat is gradually transport from the hot side to the cool side along the heat generating object.

Corresponding to the temperature field, the magnetization \mathbf{M} inside the cavity demonstrates an opposite pattern as plotted in Figs. 5(a) and 5(b). Since \mathbf{M} is everywhere parallel to the magnetic field \mathbf{H} in the flow field, Figs. 5(a) and 5(b) only display the contours of modulus of the magnetization at four planes in the cubic cavity for flows of $Gr=75$ at $Grm=1.10 \times 10^4$ and 1.96×10^4 , respectively. The modulus of \mathbf{M} is calculated directly by $M=\chi_0 H(T_c - T)/(T_c - T_0)$. As shown in Fig. 5, due to the temperature dependence of the magnetization too, the modulus of the magnetization \mathbf{M} is shown to be varied in the cavity. Large magnetization is found in the region near the upper and bottom walls, and low magnetization appears near the heat generating object.

4 Conclusions

In this article, the natural convection of a magnetic fluid in a cubic cavity with a heat generating object inside under a uniform magnetic field was simulated by the lattice

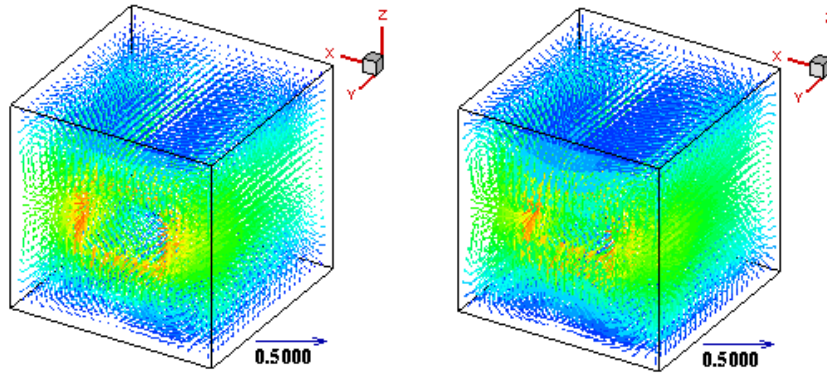


Figure 3: The velocity vectors (color plotted against temperature) of $Gr = 75$ inside the cavity at $Grm = 1.10 \times 10^4$ (left) and 1.96×10^4 (right), respectively.

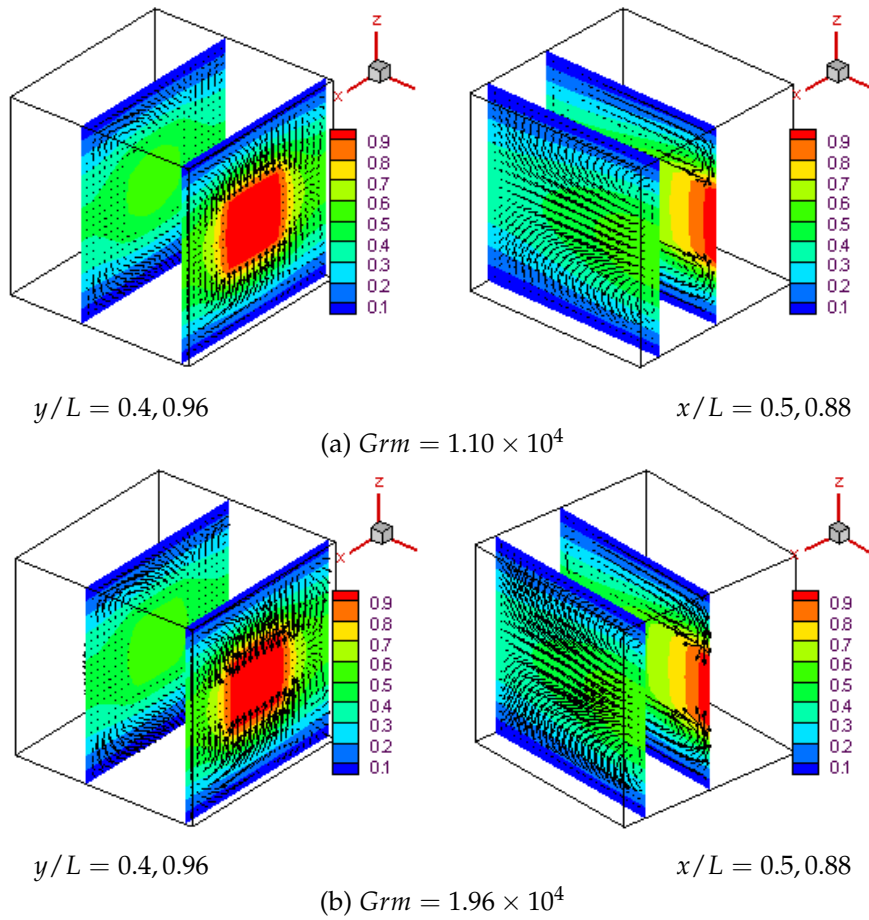


Figure 4: The temperature contours and velocity vectors of $Gr = 75$ at four planes of the cavity at $Grm = 1.10 \times 10^4$ and 1.96×10^4 , respectively.

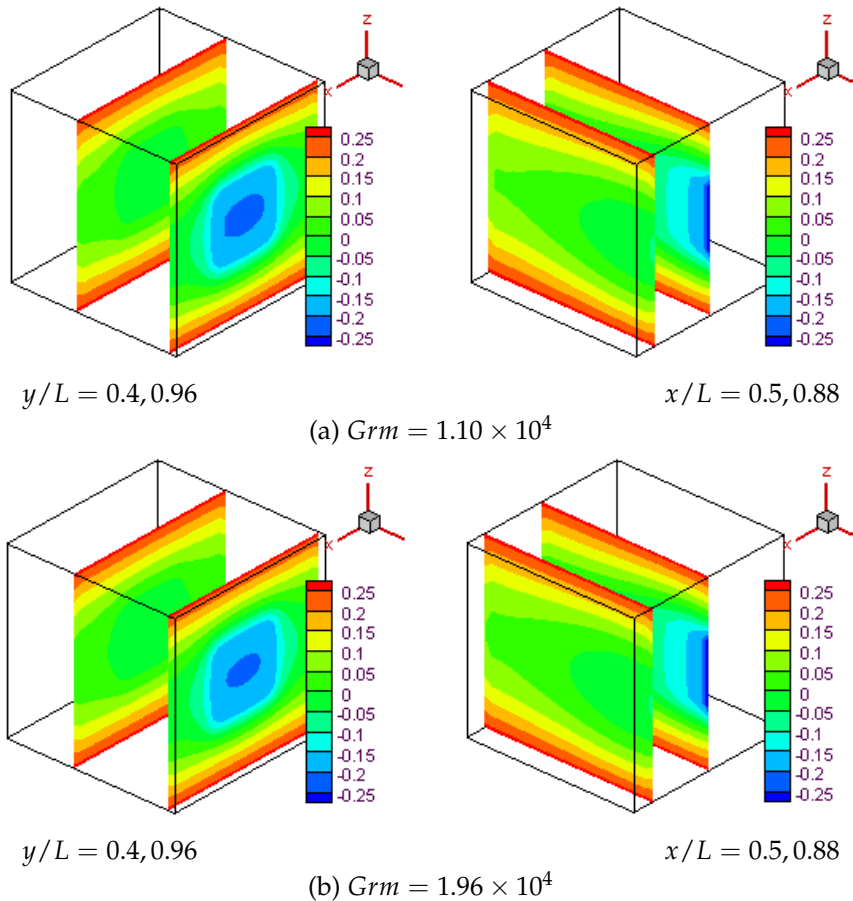


Figure 5: The contours of modulus of the magnetization M of $Gr = 75$ at four planes of the cavity at $Gr_m = 1.10 \times 10^4$ and 1.96×10^4 , respectively.

Boltzmann method. Results obtained from the present simulations are shown to be agreed well with our experimental measurements, and reveal that the magnetic and flow fields are influenced by temperature. Four symmetric weak flow rolls occur near the isolate walls in side cavity due to effects of the magnetic force, and they brings the low temperature fluid near the upper and bottom cooling walls to the region near the heat generating object, and further stream the high temperature fluid near the heat generating object to the side isolated and the upper/bottom cooling walls. With the magnetic field imposed, the heat transfer inside cavity is enhanced significantly compared to that without the magnetic field.

Acknowledgments

This work was supported by a grant-in-aid for Scientific Research (C) from the Ministry of Education, Culture, Sports, Science and Technology of Japan.

References

- [1] R. E. ROSENSWEIG, *Ferrohydrodynamics*, Cambridge University Press, London, 1985.
- [2] B. M. BERKOVSKY, *Magnetic Fluids Engineering Applications*, Oxford University Press, New York, 1993.
- [3] H. YAMAGUCHI, *Engineering Fluid Mechanics*, Springer, Netherlands, 2008.
- [4] B. A. FINLAYSON, *Convective instability of ferromagnetic fluids*, *J. Fluid Mech.*, 40 (1970), pp. 753–767.
- [5] L. SCHWAB, U. HILDEBRANDT AND K. STIERSTADT, *Magnetic Bénard convection*, *J. Magn. Magn. Mater.*, 39 (1983), pp. 113–114.
- [6] M. S. KRAKOV AND I. V. NIKIFOROV, *To the influence of uniform 456 magnetic field on thermomagnetic convection in square cavity*, *J. Magn. Magn. Mater.*, 252 (2002), pp. 209–211.
- [7] H. YAMAGUCHI, I. KOBORI, Y. UEHATA AND K. SHIMADA, *Natural convection of magnetic fluid in a rectangular box*, *J. Magn. Magn. Mater.*, 201 (1999), pp. 264–267.
- [8] H. YAMAGUCHI, I. KOBORI AND Y. UEHATA, *Natural convection of magnetic fluid in a rectangular box*, *J. Thermophys. Heat Transfer*, 13 (1999), pp. 501–507.
- [9] H. YAMAGUCHI, X.-R. ZHANG, X.-D. NIU AND K. YOSHIKAWA, *Thermomagnetic natural convection of thermo sensitive magnetic fluids in cubic cavity with heat generating object inside*, *J. Magn. Magn. Mater.*, submitted.
- [10] X. D. NIU, H. YAMAGUCHI AND K. YOSHIKAWA, *Lattice Boltzmann model for simulating temperature-sensitive ferrofluids*, *Phys. Rev. E*, 79 (2009), pp. 046713.
- [11] H. YAMAGUCHI, X.-D. NIU, X.-R. ZHANG AND K. YOSHIKAWA, *Experimental and numerical investigation of natural convection of magnetic fluids in a cubic cavity*, *J. Magn. Magn. Mater.*, submitted.
- [12] D.A. WOLF-GLADROW, *Lattice-Gas Cellular Automata and Lattice Boltzmann Models*, Springer, Berlin, 2000.
- [13] S. CHEN AND G. D. DOOLEN, *Lattice Boltzmann method for fluid flows*, *Annu. Rev. Fluid Mech.*, 30 (1998), pp. 329–364.